JOURNAL OF AIRCRAFT
Vol. 34, No. 5, September–October 1997

Method for Enhancement of the Rolling Maneuver of a Flexible Wing

N. S. Khot*
U.S. Air Force Wright Laboratory, Wright-Patterson Air Force Base, Ohio 45433
F. E. Eastep†
University of Dayton, Dayton, Ohio 45469
and
R. M. Kolonay‡
U.S. Air Force Wright Laboratory, Wright-Patterson Air Force Base, Ohio 45433

A technique for augmenting the aileron to increase the roll rates of a high-performance aircraft at high dynamic pressures for enhancement of the rolling maneuver is examined. Antisymmetric twist and camber distribution on a realistic flexible wing is determined to counteract the detrimental twisting moment of the aileron rotation to achieve recovery of the lost roll rates at high dynamic pressures. A method for prescribing the antisymmetric wing twist and camber distribution by reversing the twist and camber resulting from use of the aileron only is described. The retwisting and recambering of the wing is achieved by providing control forces obtained from a technique referred to as fictitious control surfaces. The technique of retwisting and recambering a flexible wing demonstrates a full recovery of roll rate at all dynamic pressures. Here, a full-scale realistic wing is considered for the assessment of strain energy as a measure of necessary control energy required to produce the antisymmetric twist and camber deformation on the aileron-twisted wing to recover the lost roll performance.

Nomenclature

A_f = aerodynamic stiffness matrix because of structural deformation
A_{RC} = aerodynamic stiffness matrix because of aileron rotation
A_{RP} = aerodynamic stiffness matrix because of steady roll rate
A_{RT} = aerodynamic stiffness matrix because of local angle of attack of aerodynamic panel
b = full span
C_{M_p} = roll damping stability derivative with respect to roll rate
$C_{M_{\alpha_i}}$ = aerodynamic stability derivative with respect to aerodynamic panel angle of attack α_i
C_{M_β} = aerodynamic stability derivative with respect to aileron rotation β
K = structural stiffness matrix
p = roll rate
p_{fr} = required flexible roll rate
p_{f0} = flexible roll rate because of aileron rotation of 1 deg
p_{rb} = rigid roll rate because of aileron rotation of β
p_{r0} = rigid roll rate because of aileron rotation of 1 deg
q = dynamic pressure
S = aerodynamic surface area
V_0 = freestream velocity
$\boldsymbol{x}$ = nodal displacement vector
α_R = local angle of attack of aerodynamic panel
α_{Ri} = local angle of attack of the ith aerodynamic panel
β = aileron rotation
$\Delta\varepsilon$ = change in strain energy between two deformed configurations
σ = scaling parameter

Presented as Paper 96-1391 at the AIAA/ASME/ASCE/AHS/ASC 37th Structures, Structural Dynamics, and Materials Conference, Salt Lake City, UT, April 15–17, 1996; received June 20, 1996; revision received May 29, 1997; accepted for publication June 2, 1997.

*Senior Research Aerospace Engineer, Structures Division, Flight Dynamics Directorate. Associate Fellow AIAA.
†Professor of Aerospace Engineering, Department of Mechanical and Aerospace Engineering. Associate Fellow AIAA.
‡Research Aerospace Engineer, Structures Division, Flight Dynamics Directorate. Associate Fellow AIAA.

Introduction

TO avoid destruction by a missile, the pilot of a high-performance fighter aircraft must have the capability of performing rapid turning maneuvers. Rapid turning of the aircraft requires the pilot to achieve maximum rolling of the aircraft through an aileron system by rotation of trailing-edge control surfaces of the right and left wings in a differential sense. The aileron system increases the lift on one wing and decreases lift on the opposite wing, resulting in a rolling moment producing the rolling maneuver. This is an effective technique for the generation of rolling moment for an aircraft operating in a low dynamic pressure environment where the wings can be considered as rigid. However, if the high-performance aircraft is operating at high dynamic pressures where deformation of the wing is significant, the roll rate is reduced as shown in Fig. 1 by a detrimental aerodynamic twisting moment produced by the trailing-edge control surface rotation. A roll-reversal dynamic pressure, at which the aileron system is rendered completely ineffective for producing rolling moment on a flexible wing, can be determined. Traditionally, structural designers stiffen the wings to preclude encountering the reversal dynamic pressure, but unfortunately, the additional structural weight required for stiffening results in a degradation of aircraft performance.

Rather than the traditional stiffening of wings to avoid encountering the roll reversal dynamic pressure, flexible deformation is here used as an asset rather than an impediment to be overcome, to enhance the vehicle roll performance. The flexible wing is retwisted and recambered to counteract the detrimental twisting moment produced by the aileron rotation to achieve recovery of rolling moment in a high dynamic pres-

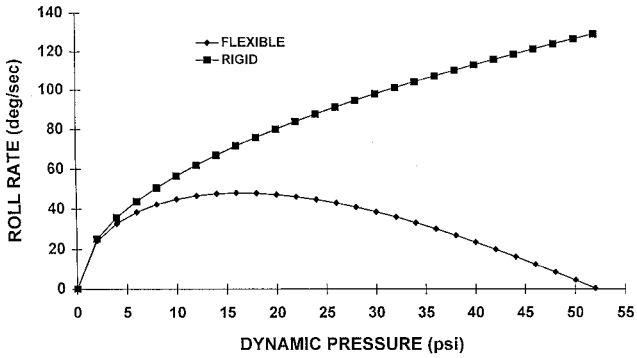

Fig. 1 Loss of roll rate because of wing flexibility.

sure environment. A method is proposed for prescribing the necessary wing twist and camber distribution to improve aileron efficiency at any dynamic pressure. An assessment of the energy requirements for retwisting and recambering of a flexible wing is made at different dynamic pressures for comparison.

One of the main elements of the flexible wing concept is rolling moment control produced by the proper wing twist and camber, which have been suggested by an internal actuation scheme,[1,2] multiple external aerodynamic control surfaces,[3,4] and strain-actuated adaptive wings.[5,6] The internal actuation scheme of the mission adaptive wing[1] did achieve aerodynamic benefits through contoured control surface deformation, but the complexity and weight penalty of the actuation system rendered the design impractical. The active flexible wing technique[3,4] using multiple control surfaces does achieve the proper wing twist for the required rolling moment and results in a decrease of structural weight by relaxing wing stiffness requirements, but the potential for an aerodynamic penalty exists. The recent developments in smart materials for controlling aircraft structural deformations make it possible to achieve the proper wing twist for controlling roll,[5] but large actuation strains were required for the aeroelastic control of realistic wings.

Presently, there are Advanced Research Projects Agency (ARPA) sponsored projects for the demonstration of the application of smart materials for twist control to improve aircraft performance, based solely on test results of small wind-tunnel models. Technology demonstration based upon wind-tunnel model tests will result in scaleup issues related to implanting smart wing technologies on an operational aircraft. Here, it is proposed that a full-scale finite element model of a realistic wing[7] be considered for proper wing twist and camber for roll control in a high dynamic pressure environment. In this way, an assessment can be made between the actuator requirements for twist control for rolling moment as compared to the conventional aileron rolling moment provided by mechanical or hydraulic actuators on a full-scale fighter aircraft. Both subsonic and supersonic design conditions were considered.

Approach

The static aeroelastic deformation in the presence of steady aerodynamic loading can be determined from the equation of equilibrium for the finite element model of the wing. This gives

$$([K] - [A_f])\{\boldsymbol{x}\} = [A_{RT}]\{\alpha_R\} + [A_{RC}]\{\beta\} + [A_{RP}]\{pb/2V_0\} \tag{1}$$

Because roll performance is the focus of this investigation, twist, camber, and control surface rotation are prescribed to be an antisymmetric function with respect to the $X-Z$ plane along the centerline of the aircraft.

The steady roll rate can be determined from the trim equation for a steadily rolling aircraft at a given dynamic pressure

$$qSb\left[\sum_{i=1}^{n} C_{M_{\alpha_i}}\alpha_{Ri} + C_{M_\beta}\beta + C_{M_p}\frac{pb}{2V_0}\right] = 0 \tag{2}$$

Aileron deflection, twist, and camber are specified to be an antisymmetric function with respect to the $X-Z$ plane of the centerline. The solution of Eq. (2) serves as a definition of aileron efficiency, (AE) given by

$$\mathrm{AE} = \frac{\left(\dfrac{pb}{2V_0}\right)}{\beta} = \frac{-\left(C_{M_\beta} + \displaystyle\sum_{i=1}^{n} C_{M_{\alpha_i}}\dfrac{\alpha_i}{\beta}\right)}{C_{M_p}} \tag{3}$$

Note that if twist and camber are neglected, Eq. (3) reduces to the familiar form for AE:

$$\mathrm{AE} = \frac{(pb/2V_0)}{\beta} = -\frac{C_{M_\beta}}{C_{M_p}} \tag{4}$$

The Unified Subsonic and Supersonic Aerodynamic Analysis code (USSAERO) (Ref. 8) was used for the computation of aerodynamic loads on the aircraft wing. This approach uses a superposition of vortex singularities applied to a discrete number of aerodynamic panels to calculate the discrete pressure distribution over the wing surface.

In this investigation, numerical calculations for aerodynamic stability derivatives, the stiffness matrix, and structural deformations are calculated from Automated Structural Optimization System (ASTROS).[9,10] Unfortunately, ASTROS will not permit an antisymmetric specification of twist and/or camber for investigating the roll problem in the roll moment trim [Eq. (2)]. To circumvent this limitation of ASTROS, a scheme referred to here as fictitious control surfaces (FCS) was instituted. To simulate flexible twist and camber, an aerodynamic panel is modeled as a control surface rotated such that the rotation angle is equal to the local angle of attack at the panel control point resulting from a wing twist and camber distribution. ASTROS does permit antisymmetric specification of control surface rotation, so that twist and camber effects can be specified in an antisymmetric fashion with this FCS.

Here, flexible twist and camber, as simulated by FCS, are specified to counter the elastic detrimental twist and camber resulting from the rotation of the aileron alone to increase the roll rate at a specified dynamic pressure. The procedure used for determining the FCS control rotations is first to find the elastic deformation, i.e., twist and camber, and flexible roll rate resulting for the specified β of the aileron only. The setting of the FCS is calculated by determining the local angle of attack at each aerodynamic panel from the aileron alone, and then reversing the angle of attack to retwist and recamber the wing. The flexible roll rate and deformation are then determined when the aileron and FCS are specified simultaneously. An increase in flexible roll-rate and aileron efficiency is given from Eq. (3).

To determine the control energy requirements necessary for the retwisting and recambering of the flexible wing using FCS, the difference in strain energy between the aileron-alone deformation and the aileron + FCS deformation is calculated. Defining $\{\boldsymbol{x}\}_{\mathrm{AE}}$ and $\{\boldsymbol{x}\}_{\mathrm{AE+FCS}}$ as the sets of structural displacements associated with the aileron alone and aileron + FCS, respectively, $\Delta\varepsilon$ between the two configurations is found by

$$\Delta\varepsilon = \tfrac{1}{2}\{\boldsymbol{x}\}^T_{\mathrm{AE+FCS}}([K] - [A_f])\{\boldsymbol{x}\}_{\mathrm{AE+FCS}} - \tfrac{1}{2}\{\boldsymbol{x}\}_{\mathrm{AE}}([K] - [A]_f)\{\boldsymbol{x}\}_{\mathrm{AE}} \tag{5}$$

where $\Delta\varepsilon$ is the control energy required for retwisting and recambering the wing to recover the lost rolling efficiency.

Design Procedure Using FCS

The FCS would introduce a set of fictitious control forces within the structural model, so that it can provide proper wing twist and camber to achieve a flexible roll rate equal to the required value at different aerodynamic pressures and flight conditions. The procedure is based on equating the rigid aileron efficiency with the aileron alone to the flexible aileron efficiency produced by the aileron + FCS. In this section, the procedure developed to determine correct rotations of the FCS to achieve desired flexible roll rate is discussed.

1) First solve the trim roll equations to calculate the flexible p_{f0} and rigid p_{r0} roll rates as a result of 1-deg rotation of the aileron for the specified dynamic pressure and Mach number.

2) Calculate the required β to obtain p_{rb} equal to p_{ft}. β is equal to p_{ft}/p_{r0}.

3) Solve the trim roll equations with aileron rotation equal to β. The rigid roll rate and flexible roll rates for this design condition would be equal to βp_{r0} and βp_{f0}, respectively. The loss of roll rate because of flexibility with aileron alone is equal to $\beta(p_{r0} - p_{f0})$.

Fit a surface spline using nodal deflections in the z direction calculated from equilibrium Eq. (1) with aileron rotation equal to β. These deflections are from the flexible aeroelastic response caused by aileron alone. In the present study, the method discussed in Ref. 11 was used for the surface spline. Calculate the slopes dw/dz from the surface spline at the midpoints of the FCS. The locations of the FCS were the same as the locations of the aerodynamic boxes. Theoretically, rotations of FCS equal to $-\tan^{-1}(dw/dz)$ should give the flexibility roll rate equal to the target roll rate p_{ft}. However, because of the approximations involved in the calculation of slopes from the spline surface fit based on the deflections, it is required to modify this distribution of rotations by multiplying them with a scale factor. The magnitude of the scale factor depends on the dynamic pressure. The scale factor was calculated by using Eq. (3) as

$$\mathrm{AE}_{\mathrm{desired}} = -\frac{\left(C_{M_\beta} + \sigma \sum_{i=1}^{n} \frac{\alpha_i}{\beta} C_{M_{\alpha_i}}\right)}{C_{M_p}} \tag{6}$$

where σ is the scale factor necessary to magnify twist and camber to achieve a desired aileron efficiency. In Eq. (6), $\mathrm{AE}_{\mathrm{desired}}$ is equal to the aileron efficiency of the rigid wing for aileron rotation equal to β in step 2 in the preceding text. Solving Eq. (6) for the scale factor at each dynamic pressure for the desired aileron efficiency gives

$$\sigma = -\frac{\beta(C_{M_\beta} + C_{M_p}\mathrm{AE}_{\mathrm{desired}})}{\sum_{i=1}^{n} \alpha_i C_{M_{\alpha_i}}} \tag{7}$$

The scaling is required because the slopes of the control surfaces are calculated from the spline function based on the displacements and not on the slopes at the structural node points. The slopes are not available from the ASTROS program. The rotations of the FCS over the aerodynamic boxes covering the fuselage area and aileron were set equal to zero, thus eliminating control forces over this region. The solution to the trim roll equations for aileron + FCS would give the flexible roll rate equal to the target p_{ft}.

Introduction of the fictitious distribution of forces within the structure using fictitious control surfaces would retwist and deform the wing so that the flexible roll rate would be equal to p_{ft}. As a measure of the amount of control energy required to retwist the wing in the presence of an airstream, the difference in the total strain energy was calculated for the two design conditions of aileron alone and aileron + FCS under trim condition using Eq. (5).

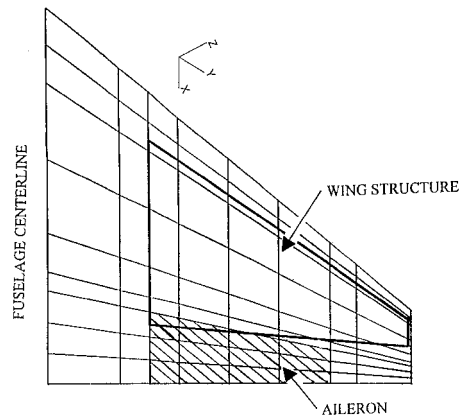

Fig. 2 Aerodynamic grid.

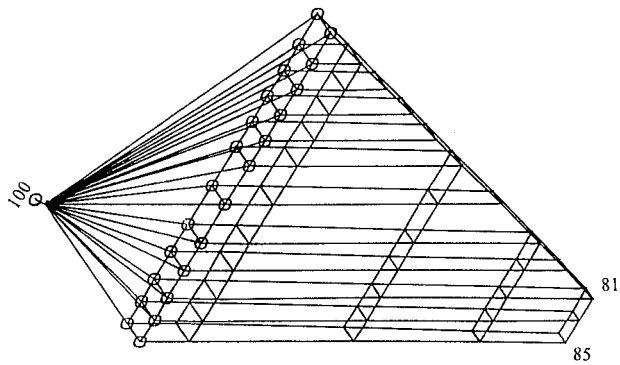

Fig. 3 Finite element model of wing structure.

Numerical Examples

A fighter-type wing was selected to be representative of a low aspect ratio wing. The wing planform is shown in Fig. 2 along with the location of the underlying structure and the aileron. In aerodynamic paneling division for this wing, special care was taken to surround the aileron hinge line and aileron edges with small panels to capture the rapid change of pressure in these locations. The wing planform was divided into nine sections along the chord and eight sections along the span, giving a total of 72 aerodynamic boxes. The aileron occupied 12 aerodynamics boxes as shown in Fig. 2. The underlying structure consisting of 10 spars and the three ribs was represented by finite elements (Fig. 3). The wing structure was idealized using 84 nodes with 54 CQUAD4, 8 CTRIA3, 62 CSHEAR, and 80 CROD elements. The fuselage was represented with node 100 at the center section. Node 100 was connected to the nodes at the base of the wing structure using CROD elements. Appropriate single- and multipoint constraints were specified for proper simulation of the wing structure connection to the fuselage. A 8000-lb mass was added at node 100 to simulate the fuselage, and a total of 1600 lb of nonstructural mass was distributed among different node points on the wing structure.

Top and bottom skins were divided into 18 areas, with all of the CQUAD4 elements within each area having the same thickness. The four specified thicknesses were equal to 0.25, 0.188, 0.08, and 0.04 in. These regions were located between the root of the wing, three ribs, and the tip of the wing. Only the translational degrees of freedom were retained associated with CQUAD4 elements. Both structural models were analyzed with aileron and aileron + FCS. For subsonic and supersonic conditions, Mach numbers 0.85 and 1.2 were selected. The design study was conducted at different dynamic pressures at sea level, starting with 5 psi. The maximum dynamic pressure was close to the aileron reversal dynamic pressure. In addition, a design study was conducted for the dy-

namic pressure equal to 30 psi, at an altitude of 15,000 ft. The required flexible roll rate for aileron + FCS was specified to be equal to 270 deg/s, at all of the dynamic pressures.

Subsonic Design Condition $M = 0.85$

The aileron reversal dynamic pressure for this design was close to 52 psi (Fig. 1). The aileron rotations to obtain a rigid rate equal to 270 deg/s at different dynamics pressures are shown in Fig. 4. The maximum required rotation was 6.73 deg at 5 psi, and the minimum was 2.13 deg at 50 psi to achieve the rigid roll rate of 270 deg/s. Figure 5 shows the change in the flexible roll rate for the two cases, aileron alone and aileron + FCS. For the aileron + FCS design condition, the flexible roll rate was equal to 270 deg/s as specified at all of the dynamic pressures. The flexible roll rate for the aileron alone was reduced from 242.14 deg/s at 5 psi to 11.01 deg/s at 50 psi. The difference between 270 deg/s and the flexible roll rate at the different dynamic pressures was the loss of roll rate because of flexibility of the wing when only the aileron was used. However, when we use aileron + FCS, the flexible roll rate was equal to the rigid roll rate for the design condition of aileron alone at the prescribed values of the aileron rotations shown in Fig. 4. Figure 6 shows the variation in aileron efficiency as a function of dynamic pressure. The flexible aileron efficiency for aileron + FCS was equal to 0.8297 at all of the dynamic pressures. This was the same as the rigid aileron efficiency when only the aileron was used. The amount of control energy required at different dynamic pressures to retwist the wing structure in the presence of an airstream, to achieve a flexible roll rate equal to 270 deg/s, is shown in Fig. 7. The control energy requirement increases from 12.58 lb at 5 psi to 2267 lb at 50 psi. To compare the relative magnitudes of the control power requirement, a static load of ± 1000 lb was applied to the wing structure at the nodes 85 and 81 at the tip. This distribution of static load was equivalent to 117 lb of strain energy. The scaling parameters calculated by using Eq. (7) for multiplying the distribution of the FCS rotations obtained from the spline fit to achieve a flexible roll rate of 270 deg/s decreased from 1.516 at 5 psi to 0.88 at 50 psi. The wing deformation patterns for the two cases for the dynamic pressure of 30 psi are shown in Fig. 8.

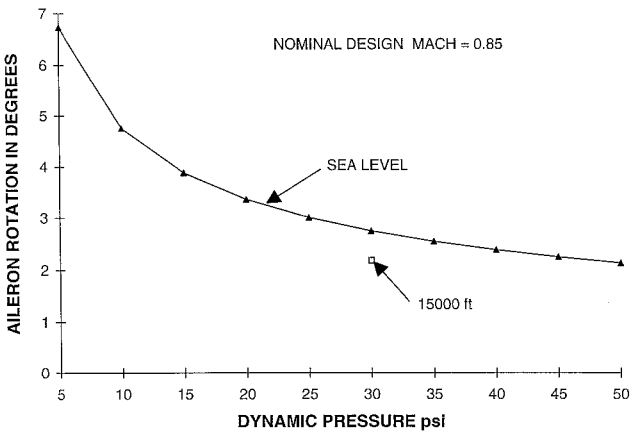

Fig. 4 Required aileron rotation to achieve rigid roll rate of 270 deg/s.

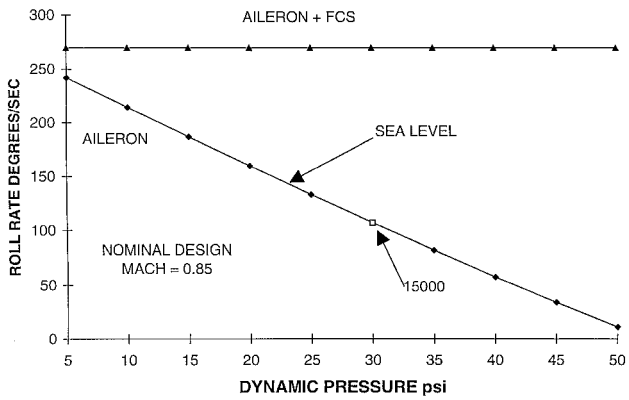

Fig. 5 Roll rate recovery using FCS.

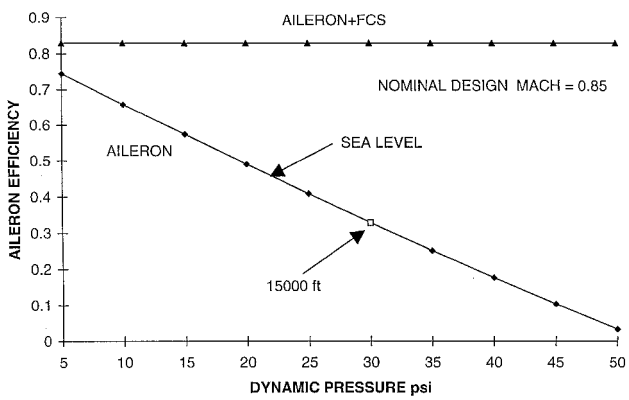

Fig. 6 Aileron efficiency recovery using FCS.

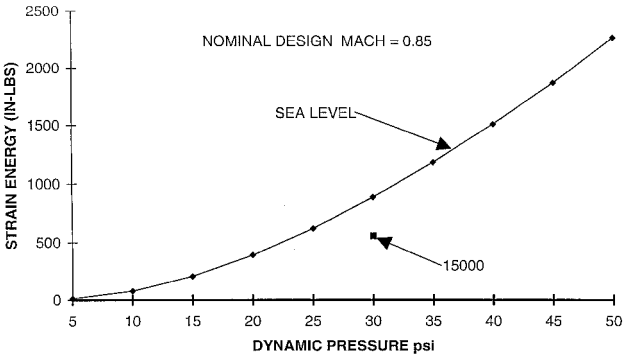

Fig. 7 Strain energy required to recover rigid roll rate of 270 deg/s.

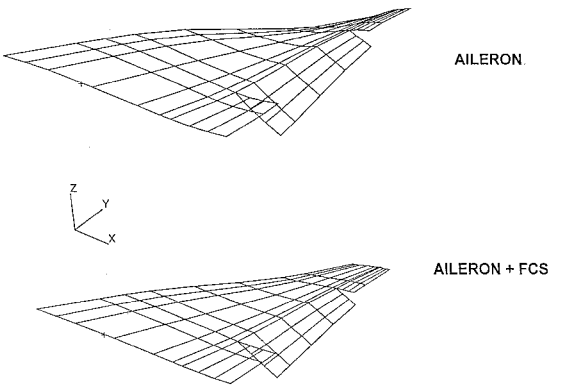

Fig. 8 Wing deformation at 30 psi (Mach = 0.85).

Supersonic Design Condition $M = 1.2$

The aileron reversal dynamic pressure for the supersonic case for the nominal design was close to 47 psi. Figure 9 shows the aileron rotations required to obtain a rigid roll rate equal to 270 deg/s at different dynamic pressures. The maximum required rotation was 12.68 deg at the aerodynamic pressure of 5 psi and the minimum was 4.22 deg at 45 psi. Figure 10 shows the change in flexible roll rate at different dynamic pressures for the two cases. The flexible roll rate was reduced from 213.85 deg/s at 5 psi to 6.509 deg/s at 45 psi when only the aileron was used. For the aileron + FCS case, the flexible

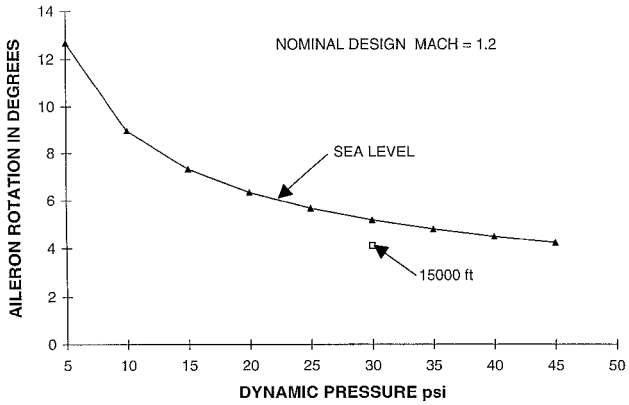

Fig. 9 Required aileron rotation to achieve rigid roll rate of 270 deg/s.

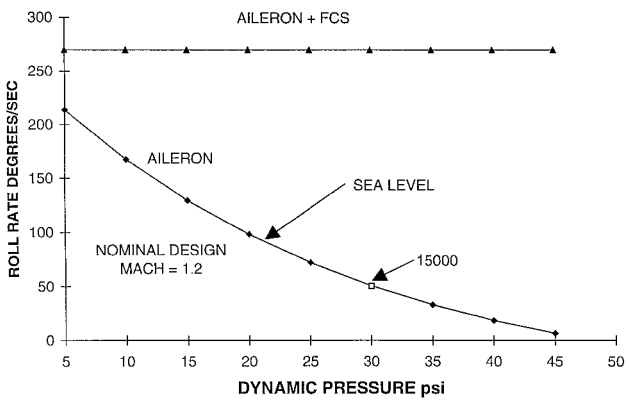

Fig. 10 Roll rate recovery using FCS.

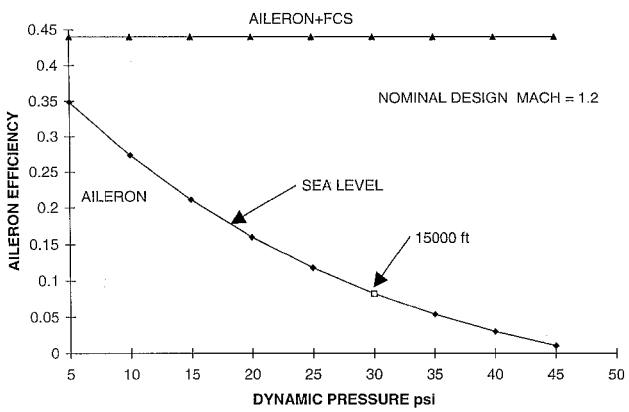

Fig. 11 Aileron efficiency recovery using FCS.

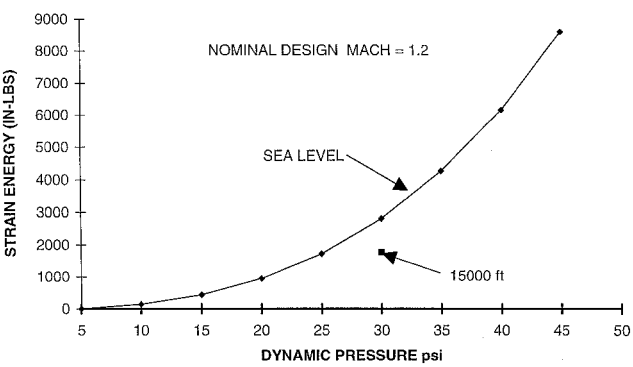

Fig. 12 Strain energy required to recover rigid roll rate of 270 deg/s.

roll rate was equal to 270 deg/s as desired at all the dynamic pressures. The variation in flexible aileron efficiency for the two design conditions, as the dynamic pressure is increased from 5 to 45 psi, is shown in Fig. 11. When only the aileron was used, the aileron efficiency was reduced from 0.3488 at 5 psi to 0.0106 at 45 psi. The flexible aileron efficiency for aileron + FCS was equal to 0.4403 at all pressure values. The amount of control energy required to deform the wing to achieve a flexible roll rate of 270 deg/s is shown in Fig. 12. This distribution for the supersonic case was substantially greater than for the subsonic case to achieve the same flexible roll rate. The values were nearly four times more at high-dynamic pressures. The scaling parameters used to multiply the FCS rotations calculated from the spline fit increased from 1.233 at 5 psi to 2.088 at 45 psi. This trend was opposite that of the subsonic case, where the scaling parameter reduced with an increase in dynamic pressure. The design condition using aileron + FCS are greater than those for aileron alone.

Conclusions

A technique for augmenting the aileron to increase the rolling moment at high dynamic pressures for enhancement of the rolling maneuver has been examined. A realistic flexible wing was twisted and cambered in an antisymmetric fashion to counteract the detrimental twisting moment of aileron rotation to achieve recovery of the lost rolling moment. A method for prescribing the antisymmetric wing twist and camber by reversing the flexible twist and camber produced by the aileron alone was described. This technique of retwisting of the wing resulted in the full recovery of the roll rate at all dynamic pressures. Here, a full-scale realistic wing was considered for the assessment of control energy for the antisymmetric twist and camber deformation on the aileron-twisted wing.

In this investigation, the flexibility of a wing was used as a departure from the traditional design procedure for wings that exhibit unacceptable roll performance. Rather than stiffening the wings, resulting in a degradation of aircraft peformance, a control scheme was designed to retwist and recamber the wing to achieve acceptable roll performance. It is anticipated that retwisting and adding camber to the aileron-twisted wing can be achieved through the use of smart materials. The data presented here will result in an assessment of the control energy requirements for twist control using smart materials or other traditional control as compared to conventional ailerons.

Acknowledgment

The second author acknowledges the support received from the Air Force Office of Scientific Research under the University Residency Research Program (URRP).

References

[1]Hall, J. W., "Executive Summary AFTI/F-111 Mission Adaptive Wing," U.S. Air Force Wright Research and Development Center, TR-89-3083, Sept. 1989.

[2]Austin, F., Knowles, G. J., Jung, W. G., Tung, E. C., and Sheedy, E. M., "Adaptive/Conformed Wing Design for Future Aircraft," 1st European Conf. on Smart Sturctures and Materials, Glasgow, Scotland, May 1992.

[3]Miller, G. D., "Active Flexible Wing (AFW) Technology," Air Force Wright Aeronautical Labs., TR-87-3036, Feb. 1988.

[4]Miller, G. D., "An Active Flexible Wing Multi-Disciplinary Design Optimization Method," *AIAA 5th Symposium on Multidisciplinary Analysis and Optimization* (Panama City, FL), AIAA, Washington, DC, 1994, pp. 1388–1394.

[5]Lazarus, K. B., Crawley, E. F., and Bohlmann, J. D., "Static Aeroelastic Control Using Strain Actuated Adaptive Structures," 1st Joint U.S./Japan Conf. on Adaptive Structures, Maui, Hawaii, Nov. 1990.

[6]Beauchamp, C. H., Nadolink, R. H., Dickinson, S. C., and Dean, L. M., "Shape Memory Alloy Adjustable Camber (SMAAC) Control Surfaces," 1st European Conf. on Smart Structures and Materials, Glasgow, Scotland, May 1992.

[7]Striz, A. G., Eastep, F. E., and Venkayya, V. B., "Influence of

Static and Dynamic Aeroelasticity Constraints on the Optimal Structural Design of Flight Vehicle Structure," *Proceedings of the AIAA 32nd Structures, Structural Dynamics, and Materials Conference* (Baltimore, MD), AIAA, Washington, DC, 1991, pp. 470–476.

[8]Woodward, F. A., "An Improved Method for the Aerodynamic Analysis of Wing-Body-Tail Configurations in Subsonic and Supersonic Flow, Part I—Theory and Application," NASA CR-2228, May 1973.

[9]Johnson, E. H., and Venkayya, V. B., "Automated Structural Optimization System (ASTROS)," *Theoretical Manual*, Vol. 1, Air Force Wright Aeronautical Labs., TR-88-3028, Dec 1988.

[10]Neill, D. J., and Herendeen, D. L., "Automated Structural Optimization System (ASTROS)," *Users Manual*, Vol. 1, TR-93-3025, March 1993.

[11]Harder, R. L., and Desmarais, R. N., "Interpolation Using Surface Splines," *Journal of Aircraft*, Vol. 9, No. 2, 1972.